Title

Pressure-induced reversal between thermal contraction and expansion in ferroelectric PbTiO3

Journal

Scientific Reports, 4(1)

ISSN

2045-2322

Authors

Zhu, Jinlong
Zhang, Jianzhong
Xu, Hongwu
et al.

Publication Date

2014

DOI

10.1038/srep03700

Peer reviewed

SCIENTIFIC REPORTS

OPEN

SUBJECT AREAS:
APPLIED PHYSICS
FERROELECTRICS AND MULTIFERROICS
MATERIALS FOR DEVICES
MECHANICAL ENGINEERING

Received
10 May 2013

Accepted
18 December 2013

Published
15 January 2014

Correspondence and requests for materials should be addressed to H.W.X. (hxu@lanl.gov); C.Q.J. (jin@iphy.ac.cn) or Y.S.Z. (Yusheng.Zhao@unlv.edu)

Pressure-induced reversal between thermal contraction and expansion in ferroelectric $PbTiO_3$

Jinlong Zhu[1,3], Jianzhong Zhang[1], Hongwu Xu[2], Sven C. Vogel[1], Changqing Jin[3], Johannes Frantti[4] & Yusheng Zhao[3,5]

[1]LANSCE, Los Alamos National Laboratory, Los Alamos, New Mexico 87545, USA, [2]EES Division, Los Alamos National Laboratory, Los Alamos, New Mexico 87545, USA, [3]National Lab for Condensed Matter Physics, Institute of Physics, CAS, Beijing, 100190, China, [4]Aalto University, School of Science, Department of Applied Physics, FI-00076 Aalto, Finland, [5]HiPSEC, Department of Physics and Astronomy, University of Nevada, Las Vegas, Nevada 89154, USA.

Materials with zero/near zero thermal expansion coefficients are technologically important for applications in thermal management and engineering. To date, this class of materials can *only* be produced by chemical routes, either by changing chemical compositions or by composting materials with positive and negative thermal expansion. Here, we report for the first time a physical route to achieve near zero thermal expansion through application of pressure. In the stability field of tetragonal $PbTiO_3$ we observed pressure-induced reversals between thermal contraction and expansion between ambient pressure and 0.9 GPa. This hybrid behavior leads to a mathematically infinite number of crossover points in the pressure-volume-temperature space and near-zero thermal expansion coefficients comparable to or even smaller than those attained by chemical routes. The observed pressures for this unusual phenomenon are within a small range of 0.1–0.9 GPa, potentially feasible for designing stress-engineered materials, such as thin films and nano-crystals, for thermal management applications.

Most materials expand on heating and contract on cooling. Although uncommon, some materials exhibit opposite behavior and possess negative coefficients of thermal expansion (CTE). There is yet a third family of materials that neither expand nor contract as temperature changes, and they display zero thermal expansion (ZTE) within a certain temperature range[1–6]. ZTE is an intriguing and useful physical attribute, because materials with ZTE do not undergo thermal shock or fatigue during rapid or repeated heating and cooling cycles, which makes them excellent candidates for applications in optics, electronics, and heat-engine components. ZTE is typically achieved by composting materials with positive and negative thermal expansion (NTE), but this route is often hindered by poor thermal stability of materials with NTE[7]. The mismatch in thermal expansion also results in internal strains in composite materials at elevated temperatures. Chemical substitution, operating as "chemical stress", is another common method to modify structural and physical properties of materials[8,9]. In ABO_3 perovskite, for example, chemical substitutions over both the A and B sites are effective pathways to tune materials with NTE or even ZTE over a large temperature range, as demonstrated by the studies in $PbTiO_3$-based pervskites[10–15]. ZTE phenomenon is also fundamentally interesting because it is associated with rich and complex physical mechanisms[1,2,4–6], such as Invar effect, valence-state transition, strain relaxation of the constituent polyhedra in crystal structures, and elastic anisotropy.

Lead titanate, $PbTiO_3$, is one of the most widely used ferroelectric and piezoelectric materials in industry[16–18]. At ambient conditions, $PbTiO_3$ possesses a tetragonal structure ($P4mm$) with an axial ratio of $c/a=1.06$[19]. The structural distortion from the ideal, cubic structure (space group $Pm3m$) is generally attributed to the covalent nature of B-O bonds in ABO_3-type ferroelectric perovskite. In tetragonal $PbTiO_3$, the $6s^2$ lone pairs effect of Pb^{2+} and the Pb-O hybridization are not only responsible for the extra degree of structural distortion[20,21], high spontaneous polarization, and relatively high Curie temperature (763 K)[22], they are also important mechanisms underlying the observed NTE[10–14,23]. The mean CTE of this compound is -1.99×10^{-5} K^{-1} over the temperature range of 300–763 K[15], and the corresponding thermal contraction is closely related to the ferroelectric soft modes with increasing temperature[15]. Above 763 K, the tetragonal $PbTiO_3$ transforms to a paraelectric cubic phase that exhibits the regular positive CTE[17,24–28].

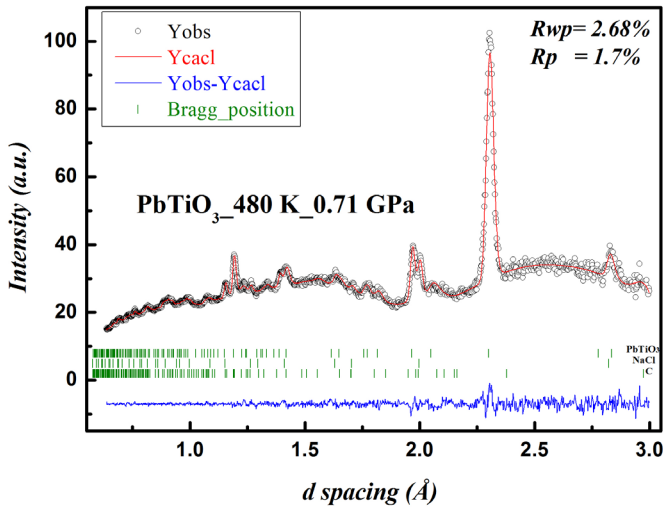

Figure 1 | A representative neutron diffraction pattern of $PbTiO_3$ collected at 480 K and 0.71 GPa. The observed and refined profiles are denoted, respectively, by open circles and red lines. NaCl is used for pressure calibration and C (graphite) is from the furnace.

As an important thermodynamic variable, pressure can effectively change the bonding characteristics (bond lengths and angles) and electron clouds overlapping of the constituent atoms in a compound, which would ultimately alter the material's structural and physical properties. In $PbTiO_3$, both tetragonality and ferroelectricity are progressively suppressed with increasing pressure at 300 K, leading to a paraelectric cubic phase at pressures above 12 GPa[29]. Compared with chemical substitution, the application of pressure is a straightforward route to tune material properties without introducing impurities and/or vacancies into the parent structure. Such defects are known to affect many properties such as structural stability, chemical diffusion, electric and ionic conductivities, and elasticity. In the present work, we applied external pressure to manipulate CTE of tetragonal $PbTiO_3$, including the achievement of near zero thermal expansion. This approach was motivated by our earlier findings[30] that at pressures above 1 GPa $PbTiO_3$ expands at all temperatures within the stability field of tetragonal phase. This behavior implies a crossover in the volumetric thermal expansion from negative to positive between ambient pressure and 1 GPa, which would presumably lead to mean ZTE over certain temperature ranges. Such pressure-tuned ZTE, if it can experimentally be verified, is not only scientifically important but also technologically relevant because similar levels of stress can readily be realized in thin-film and nanocrystalline $PbTiO_3$ produced by stress engineering[31–33].

Results

Figure 1 shows a representative neutron diffraction pattern of $PbTiO_3$ analyzed by the Rietveld method. The refined structural parameters, such as lattice parameters, atomic positions, goodness of fit and R factors, are listed in Table 1. Figure 2a shows the pressure dependence of unit-cell volumes of tetragonal $PbTiO_3$ at different temperatures. In striking contrast to the compression behavior in most materials, we observe a number of crossovers between the *P-V* isotherms within the 0–1 GPa range (Fig. 2a), implying reversals in the sign of CTE of $PbTiO_3$. At 0.1 GPa, there is a crossover point between the 300 K and 480 K volume isotherms, indicating that the mean volumetric CTE, $\overline{\alpha}_V = (V_2 - V_1)/V_1(T_2 - T_1)$, is zero over this temperature range. Similar to the behavior at ambient pressure, tetragonal $PbTiO_3$ shrinks at temperatures above 480 K with a negative CTE. The second crossover point is located at ~0.2 GPa between the 300 K and 580 K isotherms. $PbTiO_3$, however, expands with increasing temperature between 300 and 480 K and continues to contract at higher temperatures. The third crossover point is found at ~0.55 GPa between the 300 and 730 K isotherms. At this pressure, the structure expands between 300 and 580 K with essentially zero thermal expansion between 480 and 580 K isotherms; the $\overline{\alpha}_V$ is zero over the 300–730 K range due to thermal contraction between 580 and 730 K. Evidently, at a given pressure, tetragonal $PbTiO_3$ exhibits a hybrid behavior of contraction and expansion. Such unusual behavior eventually leads to three additional crossovers at higher pressures, 0.65 GPa between 480 K and 580 K isotherms, 0.85 GPa between 480 K and 730 K isotherms, and 0.9 GPa between 580 K and 730 K isotherms. When pressure is above 0.9 GPa, the unit-cell volumes expand at all experimental temperatures within the stability field of tetragonal $PbTiO_3$, which is consistent with our earlier observations using synchrotron XRD[30].

As a result of pressure-induced reversal between thermal contraction and expansion, there are mathematically an infinite number of crossover points in the *P-V-T* space, giving the infinitesimal ΔTs between two volume isotherms, where $\Delta T = T_2 - T_1$ with $T_2 > T_1$. Our findings indicate that the larger the mean temperature of T_1 and T_2, the higher the pressure is needed to produce the crossover between the corresponding isotherms (Fig. 2a). This behavior would in principle lead to mean ZTE coefficients over an infinite number of ΔTs. The exact temperature range for ZTE or near ZTE, however, cannot be determined based on the measured data because pressure varies with heating in complicated manners that depend on thermal pressure, deviatoric stress, and materials' strength. To determine the temperature ranges for ZTE, we interpolated the experimental data of Figure 2a and plot the lattice volumes as a function of temperature in Figure 2b at three constant pressures of 0.3, 0.8, and 1.2 GPa, arbitrarily chosen for clarity. Strictly speaking, there are no such temperature ranges in which $PbTiO_3$ exhibits truly zero thermal expansion (except at the "turnover" points of 447 and 556 K where CTE changes from positive to negative). In other words, CTEs would deviate from ZTE when the temperature is away from the "turnover" points. However, pressure plays a significant role in changing thermal behavior from contraction at ambient pressure to expansion above 0.9 GPa. In addition, pressure tends to elevate the temperature of turnover point, which leads to increased temperature ranges for the expansion (ΔT_{Ei}) and reduced ranges for the contraction (ΔT_{Ci}) as pressure increases. Consequently, within the 150 K range of the turnover points, the lattice volumes of $PbTiO_3$ are nearly independent of temperature. Based on such interpolated data, we calculated $\overline{\alpha}_V$ values at pressures of 0.3 GPa and 0.8 GPa, which are listed in table 2 along with those previously obtained from chemical substitutions for $PbTiO_3$-based perovskite. Strictly speaking, neither chemical nor pressure-tuned route produces thermal expansion coefficients that are truly zero. Nevertheless, the resultant CTEs are substantially smaller than those for chemically pure $PbTiO_3$ at ambient pressure. At both pressures, the pressure-tuned "*near-zero*" CTEs are comparable to or even smaller than those attained by chemical routes, indicating that pressure-tuning can be at least as effective as chemical routes for controlling materials' thermal behavior.

Discussion

In most materials, thermal expansion decreases with increasing pressure, which would in principle lead to a vanishing α at a finite pressure[34]. However, this general phenomenon does not allow the crossovers in pressure-volume isotherms. In fact, the extrapolation of experimental *P-V-T* data often requires some additional empirical constants to prevent such crossovers from occurring[35]. In the present work, we demonstrate for the first time that the *P-V* isotherms can crossover in materials with NTE at ambient pressure. The pressure-induced reversal from thermal contraction to expansion also represents a new physical route for tuning near-zero CTEs.

The pressure-tuned near-zero CTE in $PbTiO_3$ is technologically relevant to applications in thermal management and engineering.

Table 1 | The refined structural parameters of tetragonal $PbTiO_3$ and refinement agreement

Tetragonal $PbTiO_3$ Pressure/Temperature	a (Å)	c (Å)	V (Å^3)	Ti/O atom position (Z) Pb (0, 0, 0), Ti (1/2, 1/2, Z) OI (1/2, 1/2, Z) OII (1/2, 0, Z)	Refinement agreement indices
1 atm/RT	3.9154(2)	4.1622(7)	63.810(1)	Z(Ti)=0.515(3) Z(OI)=0.109(2) Z(OII)=0.615(2)	R_{wp}=3.2% R_p=1.88% R_b=5.4% χ^2=1.993
0.226 GPa/RT	3.9214(6)	4.1321(8)	63.541(2)	Z(Ti)=0.537(3) Z(OI)=0.100(2) Z(OII)=0.613(2)	R_{wp}=3.23% R_p=1.73% R_b=6.3% χ^2=1.776
0.652 GPa/RT	3.9189(7)	4.1173(10)	63.231(3)	Z(Ti)=0.538(3) Z(OI)=0.099(3) Z(OII)=0.614(2)	R_{wp}=2.76% R_p=1.79% R_b=10.12% χ^2=1.944
0.760 GPa/RT	3.9185(8)	4.1141(11)	63.171(3)	Z(Ti)=0.542(3) Z(OI)=0.089(2) Z(OII)=0.608(2)	R_{wp}=2.68% R_p=1.76% R_b=5.28% χ^2=1.833
0.858 GPa/RT	3.9180(9)	4.1093(11)	63.083(3)	Z(Ti)=0.550(3) Z(OI)=0.092(2) Z(OII)=0.610(2)	R_{wp}=2.71% R_p=1.74% R_b=5.46% χ^2=1.790
1.211 GPa/RT	3.9170(9)	4.0968(11)	62.857(4)	Z(Ti)=0.548(3) Z(OI)=0.099(2) Z(OII)=0.607(2)	R_{wp}=2.78% R_p=1.96% R_b=8.7% χ^2=1.707
1 atm/480 K	3.9360(4)	4.1155(9)	63.758(1)	Z(Ti)=0.530(3) Z(OI)=0.096(2) Z(OII)=0.606(1)	R_{wp}=4.86% R_p=1.89% R_b=7.63% χ^2=14.78
0.352 GPa/480 K	3.9315(3)	4.1142(9)	63.593(12)	Z(Ti)=0.504(5) Z(OI)=0.083(2) Z(OII)=0.599(2)	R_{wp}=3.42% R_p=1.85% R_b=10.24% χ^2=1.842
0.710 GPa/480 K	3.9319(3)	4.0962(10)	63.326(13)	Z(Ti)=0.531(5) Z(OI)=0.078(2) Z(OII)=0.598(2)	R_{wp}=2.68% R_p=1.7% R_b=8.28% χ^2=1.617
0.906 GPa/480 K	3.9282(4)	4.0965(11)	63.211(14)	Z(Ti)=0.525(5) Z(OI)=0.078(4) Z(OII)=0.596(2)	R_{wp}=2.51% R_p=1.36% R_b=4.95% χ^2=0.968
1.027 GPa/480 K	3.9281(4)	4.0926(12)	63.149(15)	Z(Ti)=0.537(5) Z(OI)=0.075(2) Z(OII)=0.593(2)	R_{wp}=2.78% R_p=1.75% R_b=9.24% χ^2=1.749
1.297 GPa/480 K	3.9281(4)	4.0792(13)	62.943(17)	Z(Ti)=0.505(5) Z(OI)=0.080(3) Z(OII)=0.590(1)	R_{wp}=2.81% R_p=2.01% R_b=14.45% χ^2=1.696
1 atm/580 K	3.9459(1)	4.0905(3)	63.690(4)	Z(Ti)=0.525(1) Z(OI)=0.084(1) Z(OII)=0.589(1)	R_{wp}=2.31% R_p=1.28% R_b=6.21% χ^2=11.95
0.434 GPa/580 K	3.9398(3)	4.0902(9)	63.490(12)	Z(Ti)=0.520(7) Z(OI)=0.067(2) Z(OII)=0.585(2)	R_{wp}=4.14% R_p=2.07% R_b=15.56% χ^2=1.811
0.784 GPa/580 K	3.9376(3)	4.0824(10)	63.297(13)	Z(Ti)=0.506(7) Z(OI)=0.071(3) Z(OII)=0.580(3)	R_{wp}=3.08% R_p=1.74% R_b=11.76% χ^2=1.455
0.940 GPa/580 K	3.9390(4)	4.0741(13)	63.213(16)	Z(Ti)=0.500(6) Z(OI)=0.075(4) Z(OII)=0.575(4)	R_{wp}=4.72% R_p=2.09% R_b=15.72% χ^2=1.962
1.080 GPa/580 K	3.9366(4)	4.0745(12)	63.141(15)	Z(Ti)=0.518(6) Z(OI)=0.070(3) Z(OII)=0.573(3)	R_{wp}=3.54% R_p=2.07% R_b=16.14% χ^2=1.797
1.361 GPa/580 K	3.9379(5)	4.0613(14)	62.979(18)	Z(Ti)= 0.517(7) Z(OI)= 0.076(4) Z(OII)=0.570(4)	R_{wp}=3.14% R_p=2.2% R_b=20.48% χ^2=1.793
1 atm/730 K	3.9580(2)	4.0534(37)	63.501(2)	Z(Ti)=0.520(1) Z(OI)=0.068(1) Z(OII)=0.570(1)	R_{wp}=2.45% R_p=1.5% R_b=10.93% χ^2=11.47
0.438 GPa/730 K	3.9557(8)	4.0462(9)	63.313(12)	Z(Ti)= 0.431(6) Z(OI)=0.062(3) Z(OII)=0.570(5)	R_{wp}=3.11% R_p=1.94% R_b=8.83% χ^2=1.726
0.856 GPa/730 K	3.9547(3)	4.0441(10)	63.246(13)	Z(Ti)=0.537(8) Z(OI)=0.071(4) Z(OII)=0.568(5)	R_{wp}=3.09% R_p=1.8% R_b=11.01% χ^2=1.477
0.978 GPa/730 K	3.9556(4)	4.0409(10)	63.227(14)	Z(Ti)=0.530(4) Z(OI)=0.077(5) Z(OII)=0.568(5)	R_{wp}=3.52% R_p=2.04% R_b=8.35% χ^2=1.781
1.109 GPa/730 K	3.9554(4)	4.0405(11)	63.214(14)	Z(Ti)= 0.524(7) Z(OI)=0.073(4) Z(OII)=0.565(5)	R_{wp}=2.96% R_p=1.84% R_b=16.85% χ^2=1.593
1.541 GPa/730 K	3.9591(6)	4.0456(15)	63.126(18)	Z(Ti)=0.523(10) Z(OI)=0.070(4) Z(OII)=0.558(7)	R_{wp}=3.2% R_p=2.11% R_b=24.77% χ^2=1.663

The required pressures for these phenomena are in a small range of 0.1–0.9 GPa, which can readily be realized in thin films and nanocrystals manufactured by stress-engineering processes. It is well known that the residual stress in thin films can be manipulated by their thickness or mismatch with substrate materials. For $PbTiO_3$ deposited on a Si(100) substrate[31], the stresses in thin films of 407 nm and 92 nm thickness are 0.96 (9) GPa and 1.77(12) GPa, respectively. They can be increased to the 1.3–2.6 GPa range when $PbTiO_3$ thin films of 400–50 nm thickness are deposited on a Pt-coated Si substrate[32]. It is well-known that in thin films the in-plane lattice parameters are constrained by the substrate materials. However, as a result of Pb-O and Ti-O bonding hybridizations, the *a* and *c* axis are coupled in the $PbTiO_3$ thin film, as demonstrated in ref [36]. Therefore, the stress can still affect the out-of-plane lattice parameter and manipulate the CTEs of $PbTiO_3$ thin films. Nano-synthesis can also introduce different levels of residual stress on the surface layer of a nanocrystal. The estimated stress in $PbTiO_3$ nanocrystals of 15 nm can be as high as 0.9 GPa based on the comparison of *c*/*a* ratios between this work and Ref. [33]. Thus, the present findings not only offer a physical route to tune near-zero CTEs in chemically-pure $PbTiO_3$ but may also potentially be useful for designing stress-engineered materials, such as thin films and nano-crystals, of desired thermal expansion coefficients, including ZTE. Last but not least, we expect that pressure-induced ZTE may occur in other NTE materials if they are structurally stable over the desired *P*-*T* space.

The thermal expansion behavior and associated ferroelectric polarization in $PbTiO_3$ perovskite are commonly linked with its tetragonality and chemical bonding. To understand the correlation between these characteristics and the present findings in the pressure-temperature space unexplored by previous studies, we look into the details of *c*/*a* ratios and hybridization between Pb and O atoms. Plotted in Figure 3a are the lattice parameters as a function of pressure for tetragonal $PbTiO_3$ at 300 K, 480 K, 580 K, and 730 K. With

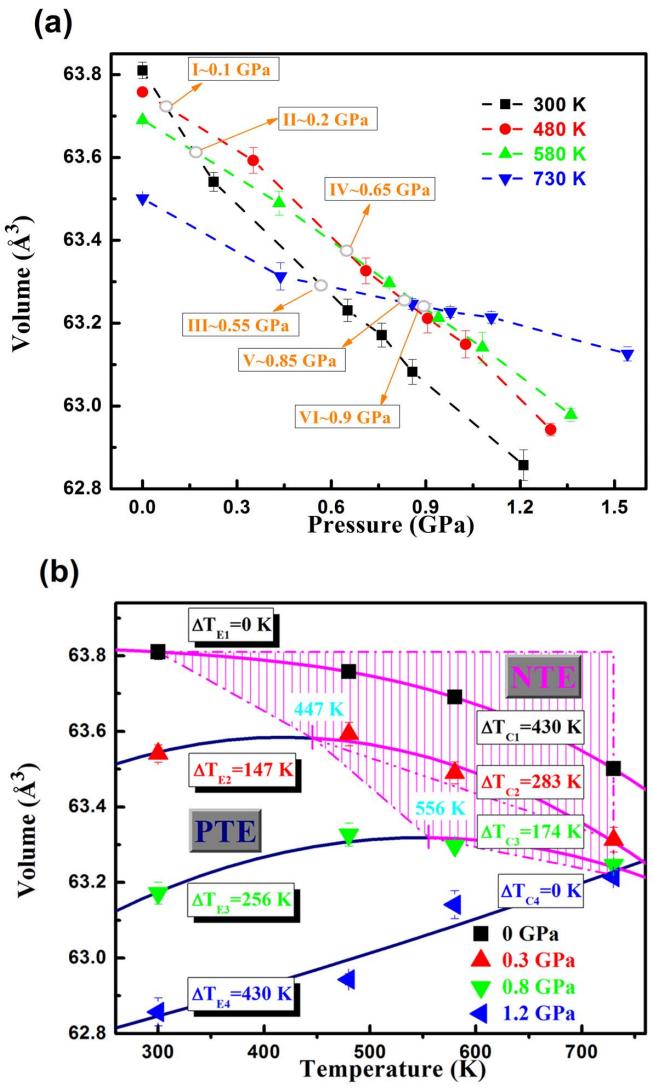

Figure 2 | (a) The pressure dependence of unit cell volumes of tetragonal $PbTiO_3$ at different temperatures. (2b), the lattice volumes of tetragonal $PbTiO_3$ as a function of temperature at constant pressures. The solid curves at 0.3 GPa, 0.8 GPa and 1.2 GPa are the data interpolated from Figure 2a. The plotted symbols are the experimental data points collected within ±0.1 GPa of the indicated pressures. The pink shadow area denotes the region of thermal contraction, and the rest plain area corresponds to the region of thermal expansion. The ΔT_{Ei} represents the temperature range for expansion and ΔT_{Ci} the temperature range for contraction. The subscripts of 1, 2, 3, and 4 in ΔT_{Ei} and ΔT_{Ci} correspond to the pressures of 0 GPa, 0.3 GPa, 0.8 GPa and 1.2 GPa, respectively. The turnover points from expansion to contraction are 447 K at 0.3 GPa and 556 K at 0.8 GPa.

increasing pressure, both lattice parameters *a* and *c* decrease (Figure 3a). However, the rate of decrease in *c* is considerably larger than that in *a*, leading to smaller *c*/*a* ratios at high pressures. Consequently, as the pressure increases, the tetragonal $PbTiO_3$ approaches the cubic structure. Figure 3a also reveals the effect of temperature on the structural distortion; at a given pressure, lattice parameter *a* increases with increasing temperature whereas *c* decreases. In addition, the magnitudes of these variations decrease with increasing pressure. Figure 3b shows that the *c*/*a* ratios are suppressed by both temperature and pressure, indicating that pressure can effectively modulate the tetragonality of $PbTiO_3$.

The thermal expansion behavior in tetragonal $PbTiO_3$ under atmospheric pressure is commonly interpreted from the symmetry argument and Pb-O bonding hybridization[37]. The first one is based on the fact that both the PbO_{12} and TiO_6 polyhedra become increasingly distorted as temperature decreases. The distortion would introduce the lattice strain[21], and as the temperature is raised and the polyhedra become more regular toward the Curie point, the unit-cell volume contracts continuously in response to the lattice strain relaxation. The second mechanism is complementary to the first one with more focus on the hybridization between the Pb 6*s* and O 2*p* states. There are two distinct atomic positions for oxygen in the structure of tetragonal $PbTiO_3$. Pb is strongly covalent with OII, while the Pb-OI bond shows ionicity. The longer Pb-OII bonds alternate with shorter Pb-OII bonds along the *c* axis, as shown in Figure 4a. It is well known that as the unequal bond lengths become equal, their average value decreases, which, in the case of $PbTiO_3$, would lead to the volume contraction as the tetragonal phase approaches the tetragonal-cubic phase transition temperature.

To gain insights into chemical bonding and associated thermal behavior at high pressure we refined the atomic positions in tetragonal $PbTiO_3$ from the collected neutron diffraction data, as summarized in Table 1. Figure 4b shows the short and long Pb-OII bond lengths as functions of pressure and temperature. At all the temperatures the two Pb-OII bonds lengths are found to approach each other with increasing pressure, which is consistent with the prediction of density functional theory computations[38]. At any given pressure, Figure 4b reveals a similar tendency of bond equalization with increasing temperature. This is not unexpected because both heating at atmospheric pressure and compression at room temperature lead to the tetragonal-cubic phase transition. In addition, at all the temperatures, the average values of short and long Pb-OII bond lengths (as well as Ti-OI bonds) show similar trends of variation of *c*/*a* ratios under pressure (Figure 3b). The observed trends for the bond-length equalization are also supported by high-pressure Raman spectroscopic data[29]. It is known that the spontaneous polarization is proportional to the square root of (*c*/*a* - 1). In Raman spectra this is reflected by the softening of the *E*(1TO) and A_1(1TO) symmetry modes[29] with increasing pressure. By symmetry, the ions vibrate in the *ab*-basal plane in *E*-symmetry modes, whereas they vibrate parallel to the *c*-axis in A_1 symmetry modes. The softening of the *E*(1TO) and A_1(1TO) modes ultimately reflects the fact that pressure weakens

Table 2 | The mean thermal expansion coefficients of $PbTiO_3$-based perovskite achieved by chemical and pressure-tuned routes. The values at 0.3 GPa and 0.8 GPa are calculated from the interpolation of experimental data in Figure 3

Compounds	CTE (°C^{-1})	Temperature range
$PbTiO_3$, ambient pressure, Ref. 15	-1.99×10^{-5}	RT-763 K
$PbTiO_3$ (0.3 GPa), this work	0.47×10^{-5}	RT-600 K
$PbTiO_3$ (0.8 GPa), this work	0.31×10^{-5}	400–700 K
0.7PT-0.3BZT, Ref. 13	-0.60×10^{-5}	RT-773 K
0.6PT-0.3BZT-0.1BF, Ref. 13	-0.31×10^{-5}	RT-773 K
$Fe[Co(CN)_6]$, Ref. 2	-0.44×10^{-5}	RT-773 K
(1-x)$PbTiO_3$-x$Bi(Ni_{1/2}Ti_{1/2})O_3$, Ref. 14	-0.88×10^{-5} (x=0.1)	RT-798 K (x=0.1)
	0.12×10^{-5} (x=0.2)	RT-798 K (x=0.2)
	0.85×10^{-5} (x=0.3)	RT-723 K (x=0.3)

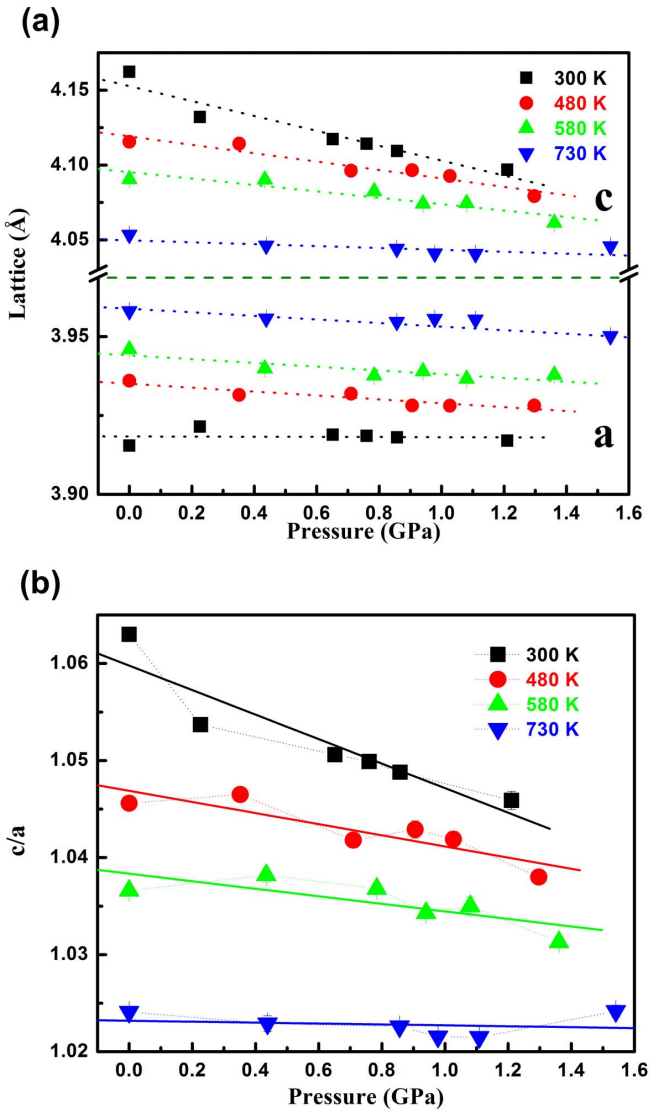

Figure 3 | (a) A Evolution of lattice parameters *a* and *c* of tetragonal $PbTiO_3$ with increasing pressure at 300 K, 480 K, 580 K and 730 K. (3b), tetragonality (*c*/*a*) of $PbTiO_3$ as functions of temperature and pressure. The solid lines are drawn from linear fitting, and the determined pressure derivatives, $d(c/a)/dP$, are −0.013(2)/GPa, −0.0057(15)/GPa, −0.0039(16)/GPa and −0.00048(107)/GPa for 300 K, 480 K, 580 K and 730 K, respectively.

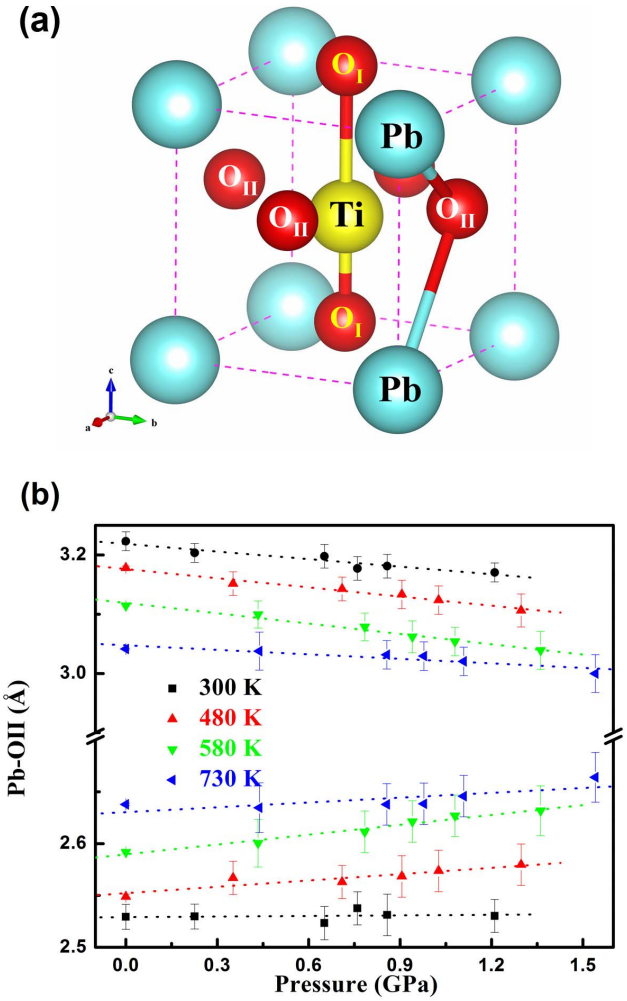

Figure 4 | (a) A schematic illustration of crystal structure for tetragonal $PbTiO_3$ showing the alternative Pb-OII and Ti-OI bonds along the *c* axis. (4b), variation of short and long Pb-OII bond lengths as functions of temperature and pressure. Similar bond equalization tendency is also observed in Ti-OI bonds. The solid lines are drawn from linear fitting to guide eyes.

the bond strength and force constants responsible for the vibration frequency, which is directly correlated to the changes in ion positions and decrease in hybridization. Thus, based on the combined observations of *c*/*a* ratios and equalization in Pb-OII bonds, the crossover behavior in volume isotherms is physically associated with tetragonality and hybridization between Pb and O atoms, which are both suppressed by pressure in tetragonal $PbTiO_3$.

Methods

We conducted high-pressure/high-temperature neutron diffraction experiments on $PbTiO_3$ using a 500-ton, toroidal anvil press (TAP-98) at the beamline of High-Pressure-Preferred-Orientation (HIPPO), Los Alamos Neutron Science Center (LANSCE). Time-of-flight neutron data were collected using detector banks at a fixed angle of $2\theta = \pm 90^\circ$. A $PbTiO_3$ powder sample was purchased from Alfa Aesar (99.9% metal based purity) and is phase-pure based on XRD. Two layers of $PbTiO_3$ and NaCl powders was first compressed into a cylindrical pallet of 5.4 mm in diameter and 7 mm in length and was then loaded into a high-*P*-*T* ceramic cell assembly specially designed for TAP-98 (see Ref [39] for detail). NaCl served as the internal pressure standard, and the Decker's equation of state (EOS) was used to calculate the pressure. Temperature was monitored by a W/5%Re-W26%Re thermocouple placed next to the sample and was stable within 25 K over a period of several hours of data acquisition time. To release the deviatoric stress built up during room-temperature compression on the polycrystalline sample, all high *P*-*T* neutron data were collected after the sample had been heated at 800 K for several minutes at each desired loading pressure. The high-temperature data at ambient pressure were collected with an ILL furnace; the sample was loaded into a vanadium can of 0.95 cm in diameter, which has low attenuation for neutrons and can hold temperatures up to 1500 K. The sample was heated under vacuum. The 144°-bank data obtained in ILL furnace and the 90°-bank data obtained in TAP-98 were used for determination of structural parameters of $PbTiO_3$ using the Rietveld method with the General Structure Analysis System (GSAS)[40].

1. Mohn, P. A century of zero expansion. *Nature* **400**, 18–19 (1999).
2. Margadonna, S., Prassides, K. & Fitch, A. N. Zero Thermal Expansion in a Prussian Blue Analogue. *J. Am. Chem. Soc.* **126**, 15390–15391 (2004).
3. Sleight, A. Materials science: Zero-expansion plan. *Nature* **425**, 674–676 (2003).
4. Zhang, Y. *et al.* Zero thermal expansion in a nanostructured inorganic-organic hybrid crystal. *Phys. Rev. Lett.* **99**, 215901 (2007).
5. Salvador, J. R. *et al.* Zero thermal expansion in YbGaGe due to an electronic valence transition. *Nature* **425**, 702–705 (2003).
6. Xu, H. *et al.* Structural mechanisms underlying near-zero thermal expansion in β-eucryptite: A combined synchrotron x-ray and neutron Rietveld analysis. *J. Mater. Res.* **14**, 3138–3151 (1999).
7. Mary, T. A. *et al.* Negative Thermal Expansion from 0.3 to 1050 Kelvin in ZrW_2O_8. *Science* **272**, 90–92 (1996).

8. Valant, M. & Davies, P. K. Crystal Chemistry and Dielectric Properties of Chemically Substituted $(Bi_{1.5}Zn_{1.0}Nb_{1.5})O_7$ and $Bi_2(Zn_{2/3}Nb_{4/3})O_7$ Pyrochlores. *J. Am. Ceram. Soc.* **83**, 147–153 (2000).
9. Moreo, A., Yunoki, S. & Dagotto, E. Phase Separation Scenario for Manganese Oxides and Related Materials. *Science* **283**, 2034–2040 (1999).
10. Xing, X. R. *et al.* Novel thermal expansion of lead titanate. *Rare Metals* **22**, 294 (2003).
11. Chen, J. *et al.* Neutron diffraction studies of structure and increasing splitting of LO-TO phonons in $Pb_{1-x}Cd_xTiO_3$. *J. Appl. Phys.* **100**, 074106 (2006).
12. Chen, J. *et al.* Structure and negative thermal expansion in the $PbTiO_3$–$BiFeO_3$ system. *Appl. Phys. Lett.* **89**, 101914 (2006).
13. Hu, P. H. *et al.* B-site Dopant Effect on the Thermal Expansion in the (1-*x*)$PbTiO_3$-*x*$BiMeO_3$ Solid Solution (Me = Fe, In, Sc). *J. Am. Ceram. Soc.* **94**, 3600–3603 (2011).
14. Hu, P. H. *et al.* Thermal Expansion, Ferroelectric and Magnetic Properties in (1 - *x*)$PbTiO_3$−*x*$Bi(Ni_{1/2}Ti_{1/2})O_3$. *J. Am. Chem. Soc.* **132**, 1925–1928 (2010).
15. Chen, J. *et al.* Zero Thermal Expansion in $PbTiO_3$-Based Perovskites. *J. Am. Chem. Soc.* **130**, 1144–1145 (2008).
16. Scott, J. F. & Paz De Araujo, C. A. Ferroelectric Memories. *Science* **246**, 1400–1405 (1989).
17. Sicron, N. *et al.* Nature of the ferroelectric phase transition in $PbTiO_3$. *Phys. Rev. B* **50**, 13168–13180 (1994).
18. Scott, J. F. Applications of Modern Ferroelectrics. *Science* **315**, 954–959 (2007).
19. Shirane, G. & Hoshino, S. On the Phase Transition in Lead Titanate. *J. Phys. Soc. Jpn.* **6**, 265–270 (1951).
20. Kuroiwa, Y. *et al.* Evidence for Pb-O Covalency in Tetragonal $PbTiO_3$. *Phys. Rev. Lett.* **87**, 217601 (2001).
21. Cohen, R. E. Origin of ferroelectricity in perovskite oxides. *Nature (London)* **358**, 136–138 (1992).
22. Glazer, A. M. & Mabud, S. A. Powder profile refinement of lead zirconate titanate at several temperatures. II. Pure $PbTiO_3$. *Acta Cryst. B* **34**, 1065–1070 (1978).
23. Kobayashi, J., Uesu, Y. & Sakemi, Y. X-ray and optical studies on phase transition of $PbTiO_3$ at low temperatures. *Phys. Rev. B* **28**, 3866–3872 (1983).
24. Burns, G. & Scott, B. A. Lattice Modes in Ferroelectric Perovskites: $PbTiO_3$. *Phys. Rev. B* **7**, 3088–3101 (1973).
25. Fontana, M. D., Hidrissi, H. & Wojcik, K. Displacive to Order-Disorder Crossover in the Cubic-Tetragonal Phase Transition of $PbTiO_3$. *Europhys. Lett.* **11**, 419–424 (1990).
26. Nelmes, R. J. *et al.* Order-disorder behaviour in the transition of $PbTiO_3$. *Ferroelectrics* **108**, 165–170 (1990).
27. Ravel, B. *et al.* Order-disorder behavior in the phase transition of $PbTiO_3$. *Ferroelectrics* **164**, 265–277 (1995).
28. García, A. & Vanderbilt, D. First-principles study of stability and vibrational properties of tetragonal $PbTiO_3$. *Phys. Rev. B* **54**, 3817–3824 (1996).
29. Sanjurjo, J. A., López-Cruz, E. & Burns, G. High-pressure Raman study of zone-center phonons in $PbTiO_3$. *Phys. Rev. B* **28**, 7260–7268 (1983).
30. Zhu, J. L. *et al.* Thermal equations of state and phase relation of $PbTiO_3$: A high P-T synchrotron x-ray diffraction study. *J. Appl. Phys.* **110**, 084103 (2011).
31. Valim, D. *et al.* Evaluating the residual stress in $PbTiO_3$ thin films prepared by a polymeric chemical method. *J. Phys. D: Appl. Phys.* **37**, 744–747 (2004).
32. Fu, D. *et al.* Thickness dependence of stress in lead titanate thin films deposited on Pt-coated Si. *Appl. Phys. Lett.* **77**, 1532–1534 (2000).
33. Akdogan, E. K. *et al.* Size effects in $PbTiO_3$ nanocrystals: Effect of particle size on spontaneous polarization and strains. *J. Appl. Phys.* **97**, 084305 (2005).
34. Birch, F. Thermal expansion at high pressures. *J. Geophys. Res.* **73**, 817–819 (1968).
35. Saxena, S. K. & Zhang, J. Thermochemical and pressure-volume-temperature systematics of data on solids, examples: tungsten and MgO. *Phys. Chem. Mineral.* 17, 45–51 (1990).
36. Janolin, P.-E. *et al.* Temperature evolution of the structural properties of monodomain ferroelectric thin film. *Appl. Phys. Lett.* **90**, 192910 (2007).
37. Sleight, A. W. Compounds That Contract on Heating. *Inorg. Chem.* **37**, 2854–2860 (1998).
38. Frantti, J. *et al.* The Factors Behind the Morphotropic Phase Boundary in Piezoelectric Perovskites. *J. Phys. Chem. B* **113**, 7967–7972 (2009).
39. Zhao, Y. *et al.* High-pressure neutron diffraction studies at LANSCE. *Appl. Phys. A* **99**, 585–599 (2010).
40. Larson, A. C. & Von Dreele, R. B. General Structure Analysis System (GSAS), *Los Alamos National Laboratory Report* LAUR 86–748 (2004).

Acknowledgments

This work was supported by the laboratory-directed research and development (LDRD) program of Los Alamos National Laboratory, which is operated by Los Alamos National Security LLC under DOE Contract No. DE-AC52-06NA25396. The experimental work has benefited from the use of the Lujan Neutron Scattering Center at Los Alamos Neutron Science Center, which is funded by the U.S. Department of Energy's Office of Basic Energy Sciences. We also acknowledge the support from NSF & MOST of China through research projects.

Author contributions

J.Z.Z., H.X., Y.Z. and C.J. conceived the work; J.L.Z. and J.Z.Z. conducted the experiments with the help of S.V.; J.L.Z. analyzed the data and drafted the manuscript; J.Z.Z., H.X., J.F. and Y.Z. helped edit the manuscript and also provided inputs for the Discussion section.

Additional information

Competing financial interests: The authors declare no competing financial interests.

How to cite this article: Zhu, J.L. *et al.* Pressure-induced reversal between thermal contraction and expansion in ferroelectric $PbTiO_3$. *Sci. Rep.* **4**, 3700; DOI:10.1038/srep03700 (2014).